Brain development is similar in Neanderthals and modern humans

Ponce de León, Marcia S ; Bienvenu, Thibaut ; Akazawa, Takeru ; Zollikofer, Christoph P E

DOI: https://doi.org/10.1016/j.cub.2016.06.022

Brain development is similar in Neanderthals and modern humans

Marcia S. Ponce de León[1]
Thibaut Bienvenu[1]
Takeru Akazawa[2]
Christoph P. E. Zollikofer[1]

[1] Anthropologisches Institut und Museum, University of Zurich, CH-8057 Zurich, Switzerland
[2] Kochi University of Technology, Kochi, 782-0003, Japan

While the braincase of adult Neanderthals was similarly capacious as that of modern humans, differences in endocranial shape suggest different brain morphologies. When and how these differences arose during evolution and development is a topic of ongoing research, with potential implications for species-specific differences in brain and cognitive development, and in life history [1, 2]. Earlier research suggested that Neanderthals followed an ancestral mode of brain development, similar to that of our closest living relatives, the chimpanzees [2-4]. Modern humans, on the other hand, were suggested to follow a uniquely derived mode of brain development just after birth, giving rise to the characteristically globular shape of the adult human brain case [2, 4, 5].

Here we re-examine this hypothesis using an extended sample of Neanderthal infants documenting endocranial development during the decisive first two years of postnatal life. The new data indicate that Neanderthals followed largely similar modes of endocranial development as modern humans (Fig. 1). These findings challenge the notion that human brain and cognitive development after birth is uniquely derived [2, 4].

We analyzed endocranial shape change from the time around birth to adulthood in a sample of N_h= 79 modern humans and N_n=15 Neanderthals (see Supplemental Table S1). The Neanderthal sample comprises the neonate from Mezmaiskaya Cave [1], two infants from Dederiyeh Cave with estimated ages at death of 1.6 and 2.0 years, respectively [1], six specimens documenting late infancy to adolescence, and six adult specimens (Table S1). Each specimen was reconstructed with computer-assisted methods, and is represented in the analyses by a range of morphologies that reflects variation resulting from independent reconstructions, and from multiple interpolations of missing regions. Endocranial form was quantified with a set of K=921 three-dimensional anatomical landmarks (see Supplemental Fig. S1A), and shape variation was analyzed with methods of geometric morphometrics (see Supplemental Materials and Methods).

Figure 1 shows that Neanderthals and modern humans have distinct endocranial morphologies already at birth. After birth, however, endocranial development in both species follows largely similar trajectories. The trajectories exhibit different early and late phases (Fig. 1A). In both species, during the early phase the cerebellar fossa, and the temporal and frontal pole regions expand with positive allometry relative to the overall endocranial surface area, while the parietal vault region expands with negative allometry (Fig. 1B). During the late phase, the cerebellar fossa and endocranial vault regions exhibit less expansion than the basal region (Fig. 1B).

Endocranial shape change during the first years of postnatal life mostly reflects changes in brain shape, because the neurocranial bones are not yet fused [3]. The pattern of early endocranial development visualized in Fig. 1B thus likely reflects substantial expansion of the cerebellum, and of the temporal and frontal cortical poles relative to other brain regions. On the other hand, the pattern of late endocranial development mostly reflects a decrease in brain growth rates during late childhood, while the cranial base continues to grow. As a result, endocranial sphericity is reduced toward adulthood (Fig. 1B) [6].

Commonalities and differences between Neanderthal and modern human modes of endocranial development permit inferences on the evolutionary history of brain development. Differences in endocranial morphology at birth reflect species-specific differences in brain and cranial development before birth, supporting earlier evidence for pervasive differences in prenatal skull development between species [1, 7]. The early postnatal mode of endocranial development, which was previously described as a uniquely human feature, is also present in the Neanderthals. It remains to be investigated whether it is a shared developmental feature of modern humans and Neanderthals already present in their last common ancestor (LCA), or whether it was not present in the LCA, and evolved in parallel in Neanderthals and modern humans.

While early postnatal changes in endocranial shape are a proxy of brain development, the increase in endocranial volume (ECV) is a proxy of brain growth. Tracking ECV expansion from birth to adulthood indicated that Neanderthals and Late Pleistocene modern humans followed largely similar brain growth trajectories [1]. Combining the evidence on brain growth [1] and brain development (this study), we conclude that postnatal brain ontogeny was largely similar in Neanderthals and coeval modern human populations. These findings are in contrast with previous studies [2, 4], which proposed species-specific differences in early postnatal brain development, and possible differences in cognitive development between Neanderthals and modern humans. The data provided here do not support this hypothesis, and are most parsimoniously interpreted as evidence for similar brain development, and similar cognitive development in Neanderthals and modern humans.

It is worth considering the potential significance of Neanderthal-modern human similarities in brain and cognitive development in the light of genetic evidence for interbreeding across species boundaries [8]. Early brain and cognitive development is substantially influenced by an infant's socio-cultural environment [9]. Similar modes of brain and cognitive development in Neanderthals and modern humans might thus have facilitated the behavioral integration of Neanderthal-modern human offspring in their human "host" groups, ultimately facilitating the introgression of Neanderthal alleles into the modern human gene pool [8]. Further research will be required, however, to test this hypothesis with genomic and archeological evidence documenting the complex spatiotemporal patterning of Neanderthal-modern human interactions [8, 10].

Figure Legend

Figure 1. Neanderthal and modern human endocranial development.

(**A**) Developmental trajectories through shape space (the first two principal components, PC1 and PC2, account for 47% of total shape variation in the sample). Green: modern humans. Polygons and labels indicate range of variation and mean values, respectively, for consecutive age classes (A: preterm fetus; B: neonate; C/D: incomplete/complete deciduous dentition; E/F/G: first/second/third molar erupted). Green arrows approximate early (neonate to infant) and late (infant to adult) phases of ontogeny. Red: Neanderthals. Labels represent individual specimens (Mez: Mezmaiskaya neonate; De1/De2: Dederiyeh 1 and 2 infants; Sub: Subalyuk 2; Roc: Roc de Marsal; Gi2: Gibraltar 2; Eng: Engis 2; Tes: Teshik Tash; Mou: Le Moustier 1; Gi1: Gibraltar 1; Amu: Amud 1; Tab: Tabun 1; Sp1/Sp2: Spy 1/2; Gua: Guattari 1; see Table S1 for individual ages). Each Neanderthal specimen is represented by a set of reconstructive variants (polygons). Red arrows indicate early and late phases of ontogeny. Gray arrows indicate difference between neonates of Neanderthals and modern humans. See also Figure S1B.

(**B**) Patterns of endocranial shape transformation corresponding to the arrows in graph A. Shape change from neonate to infant, and from infant to adult morphologies in Neanderthals (*H. n.*; red) and modern humans (*H. s.*; green). Gray arrows: difference between neonate modern human and Neanderthal endocrania. Yellow/blue hues indicate the amount of local surface change (positive/negative deviation from isometric expansion) required to reach the endocranial morphology at the tip of the arrow from the morphology at the base of the arrow. Note that species-specific differences in endocranial morphology are present already at birth, but that patterns of postnatal endocranial development are largely similar in both species. See also Figure S1C.

References

1. Ponce de León, M.S., Golovanova, L., Doronichev, V., Romanova, G., Akazawa, T., Kondo, O., Ishida, H., and Zollikofer, C.P.E. (2008). Neanderthal brain size at birth provides insights into the evolution of human life history. Proc Natl Acad Sci USA *105*, 13764-13768.
2. Gunz, P., Neubauer, S., Maureille, B., and Hublin, J.-J. (2010). Brain development after birth differs between Neanderthals and modern humans. Curr Biol *20*, R921-R922.
3. Neubauer, S., Gunz, P., and Hublin, J.-J. (2010). Endocranial shape changes during growth in chimpanzees and humans: A morphometric analysis of unique and shared aspects. J Hum Evol *59*, 555-566.
4. Gunz, P., Neubauer, S., Golovanova, L., Doronichev, V., Maureille, B., and Hublin, J.-J. (2012). A uniquely modern human pattern of endocranial development. Insights from a new cranial reconstruction of the Neandertal newborn from Mezmaiskaya. J Hum Evol *62*, 300-313.
5. Bruner, E., Manzi, G., and Arsuaga, J.L. (2003). Encephalization and allometric trajectories in the genus *Homo*: Evidence from the Neandertal and modern lineages. Proc Natl Acad Sci USA *100*, 15335-15340.
6. Scott, N., Neubauer, S., Hublin, J.-J., and Gunz, P. (2014). A shared pattern of postnatal endocranial development in extant hominoids. Evol Biol *41*, 572-594.
7. Ponce de León, M.S., and Zollikofer, C.P.E. (2001). Neanderthal cranial ontogeny and its implications for late hominid diversity. Nature *412*, 534-538.
8. Fu, Q., Posth, C., Hajdinjak, M., Petr, M., Mallick, S., Fernandes, D., Furtwangler, A., Haak, W., Meyer, M., Mittnik, A., et al. (2016). The genetic history of Ice Age Europe. Nature, doi: 10.1038/nature17993.
9. Klingberg, T. (2014). Childhood cognitive development as a skill. Trends Cog Sci *18*, 573-579.
10. Higham, T., Douka, K., Wood, R., Ramsey, C.B., Brock, F., Basell, L., Camps, M., Arrizabalaga, A., Baena, J., Barroso-Ruiz, C., et al. (2014). The timing and spatiotemporal patterning of Neanderthal disappearance. Nature *512*, 306-309.

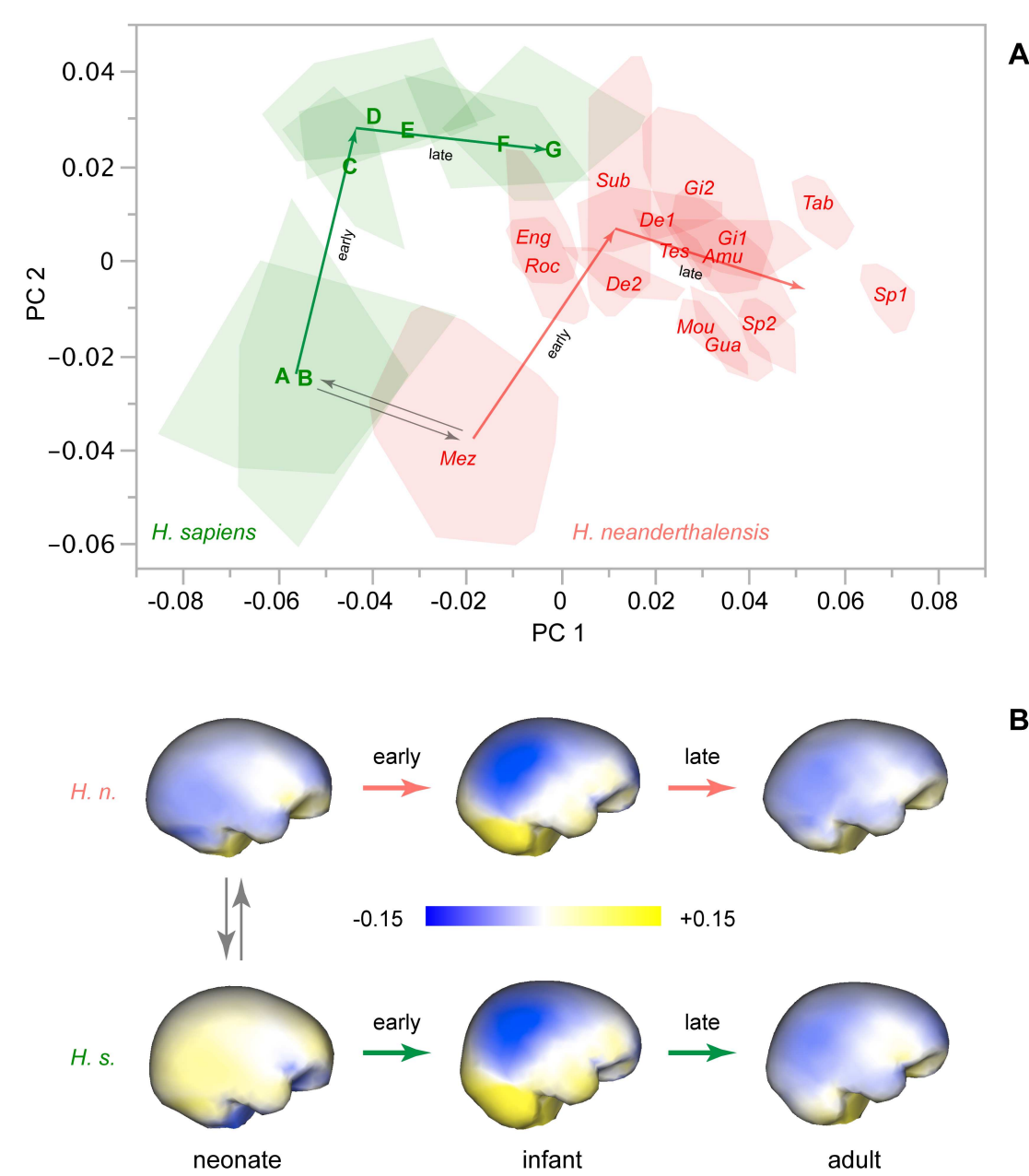
A
0.04
0.02
0
−0.02
−0.04
−0.06
PC 2
-0.08
-0.06
-0.04
-0.02
0
0.02
0.04
0.06
0.08
PC 1
A
B
C
D
E
F
G
early
late
Sub
Gi2
Tab
De1
Eng
Gi1
Tes
Amu
Roc
De2
Sp1
Mou
Sp2
Gua
Mez
H. sapiens
H. neanderthalensis
B
H. n.
H. s.
early
late
-0.15
+0.15
neonate
infant
adult

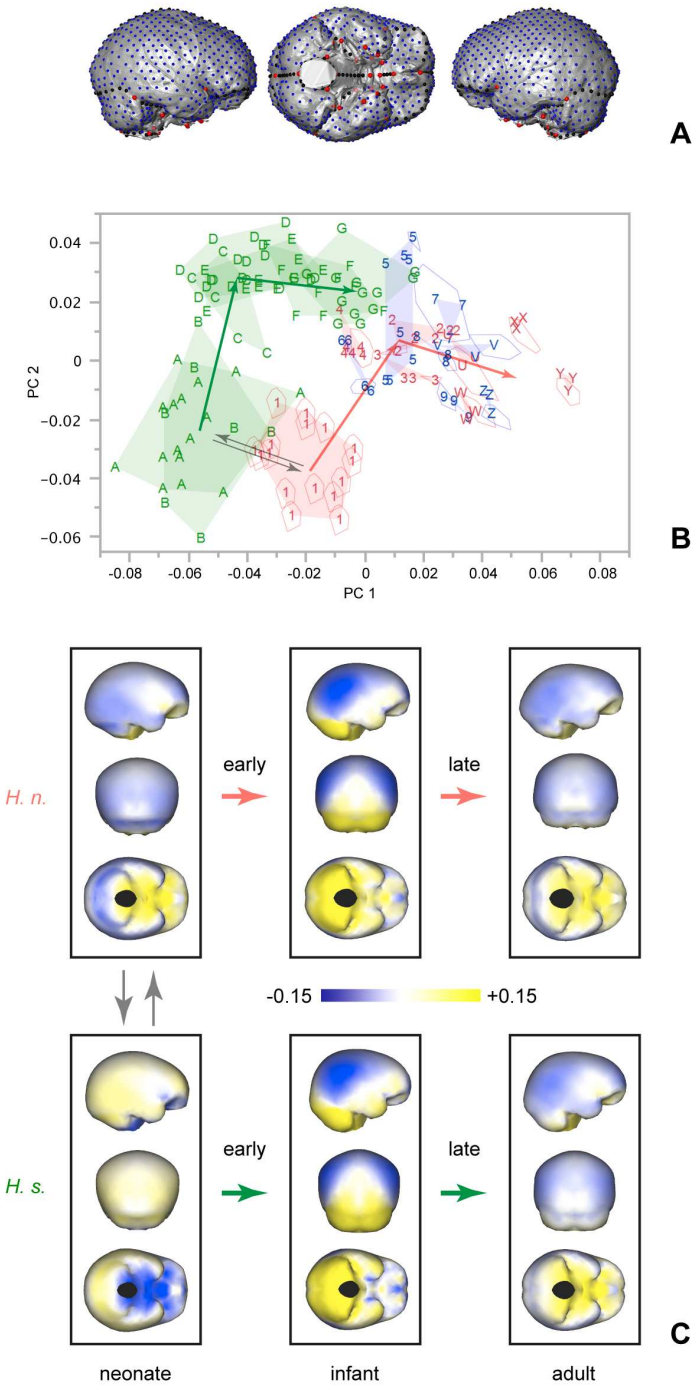

Figure S1. Related to Figure 1.

(**A**) Endocranial landmarks used for geometric morphometric analyses. Red: fixed landmarks; black: curve semilandmarks; blue: surface semilandmarks.

(**B**) Extended version of Figure 1A. Patterns of interindividual and intraindividual variation of endocranial shape (same data as in Fig. 1A). Green symbols: modern humans. Letters indicate endocranial shape of individual modern human specimens representing age groups A-G (see Table S1); filled polygons are convex hulls drawn around age groups. Red and blue symbols: Neanderthals (the two colors are only used to disambiguate overlapping specimens). Filled polygons indicate variation among independent virtual reconstructions of one and the same specimen (specimens are identified by numbers 1-9 and letters U-Z). Outlined polygons represent the range of variation resulting from interpolation of missing regions in a given virtual reconstruction of a Neanderthal specimen (data represented for a subset of reconstructions).

(**C**) Extended version of Fig. 1B. Patterns of endocranial shape transformation along the arrows indicated in graph S1B.

Table S1. Sample structure.

A: modern humans		
group	*age class*	*N*
pre-term	A	16
neonate	B	7
incomplete deciduous	C	6
complete deciduous	D	17
M1 erupted	E	10
M2 erupted	F	9
M3 erupted	G	14

B: Neanderthals			
specimen	*age class*	*individual age*	*reference*
Mezmaiskaya	B	1-2 weeks	[S1]
Dederiyeh 1	C	1.6 years	[S1]
Dederiyeh 2	C	2.0 y	[S1]
Engis 2	D	3.0 y	[S2]
Subalyuk 2	D	3.2 y	[S3]
Roc de Marsal	D	4.5 y	[S2]
Gibraltar 2	D	4.6 y	[S2]
Teshik Tash	E	8.0 y	[S3]
Le Moustier 1	F	11.6-12.1 y	[S2]
Amud 1	G	adult	
Gibraltar 1	G	adult	
Guattari	G	adult	
Tabun 1	G	adult	
Spy 1	G	adult	
Spy 2	G	adult	

Supplemental Materials and Methods

The modern human (*H. sapiens*) sample consists of *N*=79 crania representing cross-sectional ontogenetic series from preterm fetuses to adults (Table S1A). Specimens were grouped according to their maxillary dental eruption stage: preterm fetus (stage A), neonate (B), incomplete/complete deciduous dentition (C/D), first/second/third permanent molars fully erupted (E/F/G). Subsamples representing neonate to early postnatal ontogeny mostly consist of wet-preserved specimens (frozen, formalin/alcohol), which exhibit only minor deformation and/or shrinkage compared to dry skeletal specimens, thus minimizing potential deformation bias. Males and females are represented in similar proportions throughout the sample. Specimens are from the Collections of the Anthropological Institute and Museum of the University of Zurich, the Anatomical Institute of the University of Zurich, the University Children's Hospital Zurich, the University Hospital Leuven, the Natural History Museum London, and the Kyoto University Anatomical Collections, and represent a mixed-population sample. The Neanderthal sample consists of *N*=15 specimens representing neonate to adult stages (Table S1B).

Volumetric data of all crania were acquired with computed tomography (CT), using beam collimations between 0.5 and 1.0 mm, and performing cross-sectional reconstructions with voxel sizes between 0.2^3 and 0.5^3 mm. For each cranium, the endocranial surface was digitally extracted from the CT data volume following procedures described in [S4], and using the softwares Avizo and Geomagic Studio. Endocranial volumes (ECV) were evaluated from the surface data using the software Avizo.

For each Neanderthal specimen several independent CT-based virtual reconstructions were performed to obtain a range of possible morphologies [S5]. Wherever possible, regions missing on one side were completed by mirror-imaged parts preserved on the other side. Endocranial landmarks (Fig. S1A) were positioned on the reconstruction, and landmark locations corresponding to missing regions on both sides of the endocast were completed with thin-plate spline (TPS) interpolation methods [S6]. These procedures take into account two sources of reconstructive variation: a) variation among multiple independent anatomical reconstructions, and b) variation among multiple interpolations of missing regions.

Endocranial (EC) morphology was quantified with *K*=921 three-dimensional anatomical landmarks (LMs), which are distributed equally over the entire surface of the endocast, and represent fixed LMs (K_p=27), curve semilandmarks (SLMs) (K_c=110), and surface SLMs (K_s=784) (Fig. S1A). Fixed LMs and curve SLMs were acquired with Avizo. Curves were defined manually as cubic splines with densely spaced nodes between fixed endpoints, and equidistant curve SLMs were sampled along the splines. A template of regularly-spaced surface SLMs was defined for one specimen, then warped to every other specimen, using the fixed LMs and curve SLMs as nodes of a TPS interpolation function, and projecting the warped surface SLMs onto the target specimens along endocranial surface normals. To optimize the position of SLMs and establish geometric correspondence across all specimens of the sample, the curve SLMs were allowed to slide along tangents to the curves, and the surface SLMs along tangents to the surface [S7]. Sliding was iterated until convergence to the minimum bending energy criterion [S8]. Since natural patterns of left-right asymmetry are not considered here, all specimens were symmetrized via relabeled reflection of landmarks. Finally, Generalized Procrustes analysis (GPA) was applied to minimize differences in scale, position and orientation between the specimens' landmark configurations. Principal component analysis (PCA) was used to reduce the dimensionality of shape space and visualize major patterns of shape variation in the sample. All procedures were performed with the R package Morpho [S9].

Actual physical patterns of endocranial shape change were visualized using color-mapping methods described earlier [S10]. Since endocranial volumes and surfaces increase along the entire developmental trajectory, endocranial shape change is visualized in terms of positive versus negative allometric expansion (allometric exponents >1 versus <1) of local regions of the endocranial surface. This method provides a coordinate-free representation of shape transformation, which is independent of the Procrustes registration used to superimpose source and target morphologies. The resulting patterns hint at local changes in relative endocranial surface area, and potentially in relative surface area of the underlying brain structures.

Supplemental Results

Interpretation of the results of PCA

PCA is a statistical technique to reduce the dimensionality of multivariate data, and to explore principal patterns of shape variation in the sample in a low-dimensional version of multivariate space, as defined by the first few principal components (PCs). In our analyses, the first 6 PCs account for 73% of total

variation of the sample (PC1: 32%, PC2: 15%, PC3: 9%, PC4: 8%, PC5: 6%, PC6: 3%). Considering that PCs are statistical rather than biological entities, they are used here with the only purpose of visualizing principal patterns and magnitudes of shape variation among and within species, age groups, and reconstructive variants of fossil specimens (Figs. 1A and S2B). Actual physical patterns of endocranial shape change (Figs. 1B and S2C) are based on group-specific mean shapes, which represent the shape information comprised in all PCs.

Comparison of the directions of ontogenetic trajectory segments

While color-mapping procedures permit direct visual comparison of Neanderthal and human patterns of endocranial shape change (Figs. 1B and S1C), we also compared directions of developmental trajectory segments through shape space (Fig. 1A and S1B) using the methods proposed in ref. [S11]. The three hypotheses to test here were as follows: (1) early and late ontogenetic trajectories have different directions through shape space, both for Neanderthals and modern humans; (2) early trajectories of Neanderthals and modern humans have similar directions through shape space; (3) late trajectories of Neanderthals and modern humans have similar directions through shape space. To test these hypotheses the sample was subdivided, for each species, into two subgroups, "early development" (preterm, neonate, incomplete/complete deciduous dentition) and "late development" (complete deciduous dentition, M1, M2, M3) (note that the “complete deciduous dentition” stage represents the oldest stage of the “early development” group, and the youngest stage of the “late development” group). For each species and each group, a trajectory segment vector was evaluated by multivariate regression of endocranial shape on age class. Divergence between pairs of group-specific vectors was evaluated statistically by 1000 random samplings of 20 specimens from the pooled-group sample (reconstructive variants of Neanderthal specimens were treated as specimens). Results show significant directional differences between early and late trajectory segments in both Neanderthals (divergence angle φ=92.9º; p=0.012) and modern humans (φ=88.5º; p=0.009). On the other hand, early trajectories of both species exhibit similar directions (φ=26.9º; p=0.333), and late trajectories exhibit similar directions as well (φ=26.6º; p=0.437).

Comparison of methods and results of this study with previous studies

Previous analyses suggested that endocranial morphologies of Neanderthals and modern humans were largely similar at birth, but that species-specific modes of endocranial development diverged after birth, with humans exhibiting a uniquely derived mode of development [S12, S13]. In contrast with these findings, the present study indicates substantial endocranial differences between species at birth, but largely similar modes of endocranial development after birth. Several factors might explain the different outcomes of these studies.

- *Sparse and fragmentary evidence from young Neanderthal infants.* Reconstruction of the early phase of postnatal endocranial development in Neanderthals in previous studies [S12, S13] relied on two neonate specimens (Le Moustier 2 and Mezmaiskaya 1), and a single infant specimen (Pech de l’Azé) with an estimated age at death of 2.2 years. Reconstructed endocranial shapes of all three specimens were largely similar. The reported neonate-infant endocranial similarity [S12, S13] might represent a reconstruction effect (in the Pech de l'Azé specimen, the posterior cranial fossa is only partially preserved, but it is a key region to characterize early postnatal endocranial development). Alternatively, the results of refs. [S12, S13] might represent a sampling effect: in modern humans there is overlap in endocranial shape variation between neonates and young infants, and similar overlap might have existed in the Neanderthals. Overall, thus, the evidence for endocranial shape variation in Neanderthal infants was both sparse and fragmentary. – The Dederiyeh infants (1.6 and 2.0 years) fill this data gap, and indicate that endocasts of young Neanderthal infants were different from those of neonates (Figs. 1, S1).
- *Methods of virtual fossil reconstruction.* The methods of reconstruction used in previous studies [S6] account for variation in the interpolation of missing regions in a given virtual reconstruction, but do not account for variation resulting from alternative virtual reconstructions. As shown in Fig. S1B, the amount of variation among independent virtual reconstructions is often larger than the amount of variation represented by different interpolations of the missing endocranial regions of a given reconstruction. This effect is considered here during the comparison of ontogenetic trajectories.
- *Landmark sampling density.* Endocranial shape is quantified here with K=921 anatomical landmarks (compared with K=307 landmarks in previous analyses [S12, S13]). The denser sampling scheme permits better discrimination between group-specific endocranial morphologies. Overall, our data indicate that Neanderthal endocranial development followed a two-phase ontogenetic trajectory similar to that of modern humans (as first described in [S14]). However, the

Neanderthal trajectory occupies a different location in shape space, indicating substantial differences in endocranial shape already at birth, which persist throughout postnatal ontogeny.

- *Visualization of shape change.* Endocranial shape change and shape difference was visualized previously with TPS interpolation grids between "source" and "target" shapes, and with source-target comparisons of individual specimens, visualized as "heat maps" [S12, S13]. The outcome of the latter visualization procedure is sensitive to methods of source-target superposition, and to the choice of individual specimens. Furthermore, the use of 2D-TPS grids for the visualization of 3D-shape change has been discouraged because "transformation grids render the space between the landmarks, precisely where no data are available" (ref. [S15], p. 21). The method used here [S10] circumvents both limitations: it is independent of superposition procedures, and it visualizes shape change on the surface defined by the anatomical landmarks used for the geometric morphometric analyses.
- *Statistical comparison of species-specific ontogenetic trajectories.* Differences between Neanderthal and modern human endocranial developmental trajectories have been evaluated previously with forward and backward simulation strategies [S12, S13]. To this end, a human-like developmental trajectory was applied backwards to adult Neanderthal morphologies, and a truncated human-like trajectory was applied forwards to neonate human morphologies. The simulated outcomes (neonates/adults) were then compared with actual neonate/adult Neanderthal morphologies. This method has several drawbacks. As has been shown earlier, evolutionary developmental shifts between species cannot be modeled straightforwardly by shifts of entire developmental trajectories in shape space [S16]. Furthermore, endocranial ontogeny reflects the combined effects of brain development and the development of the cranial base and face [S17, S18], such that forward/backward simulations tend to conflate the potential effects of species-specific differences in brain development, and in basicranial and facial development. Comparison of the direction of trajectory segments [S11] is a more focused procedure, which permits to differentiate between the major factors mediating endocranial shape change (early phase: dominant effects of brain growth and development; late phase: dominant effects of basicranial and facial growth and development).

Supplemental References

S1. Ponce de León, M.S., Golovanova, L., Doronichev, V., Romanova, G., Akazawa, T., Kondo, O., Ishida, H., and Zollikofer, C.P.E. (2008). Neanderthal brain size at birth provides insights into the evolution of human life history. Proc Natl Acad Sci USA *105*, 13764-13768.

S2. Smith, T.M., Tafforeau, P., Le Cabec, A., Bonnin, A., Houssaye, A., Pouech, J., Moggi-Cecchi, J., Manthi, F., Ward, C., Makaremi, M., et al. (2015). Dental ontogeny in Pliocene and Early Pleistocene hominins. PLoS One *10*, e0118118.

S3. Ponce de León, M.S., and Zollikofer, C.P.E. (2001). Neanderthal cranial ontogeny and its implications for late hominid diversity. Nature *412*, 534-538.

S4. Bienvenu, T., Guy, F., Coudyzer, W., Gilissen, E., Roualdès, G., Vignaud, P., and Brunet, M. (2011). Assessing endocranial variations in great apes and humans using 3D data from virtual endocasts. Am J Phys Anthropol *145*, 231-246.

S5. Zollikofer, C.P.E., and Ponce de León, M.S. (2005). Virtual reconstruction: A primer in computer-assisted paleontology and biomedicine, (New York: Wiley).

S6. Gunz, P., Mitteroecker, P., Neubauer, S., Weber, G.W., and Bookstein, F.L. (2009). Principles for the virtual reconstruction of hominin crania. J Hum Evol *57*, 48-62.

S7. Gunz, P., Mitteroecker, P., and Bookstein, F.L. (2005). Semilandmarks in three dimensions. In Modern Morphometrics in Physical Anthropology, D.E. Slice, ed. (Springer), pp. 73-98.

S8. Bookstein, F.L. (1996). Applying landmark methods to biological outline data. In Image Fusion and Shape Variability Techniques. (Leeds: Leeds University Press), pp. 59-70.

S9. Schlager, S. (2014). Morpho: Calculations and visualisations related to Geometric Morphometrics. http://sourceforge.net/projects/morpho-rpackage.

S10. Zollikofer, C.P.E., and Ponce de León, M.S. (2002). Visualizing patterns of craniofacial shape variation in *Homo sapiens*. Proc. Roy. Soc. B *269*, 801-807.

S11. Collyer, M.L., and Adams, D.C. (2013). Phenotypic trajectory analysis: comparison of shape change patterns in evolution and ecology. Hystrix *24*, 75-83.

S12. Gunz, P., Neubauer, S., Maureille, B., and Hublin, J.-J. (2010). Brain development after birth differs between Neanderthals and modern humans. Curr Biol *20*, R921-R922.

S13. Gunz, P., Neubauer, S., Golovanova, L., Doronichev, V., Maureille, B., and Hublin, J.-J. (2012). A uniquely modern human pattern of endocranial development. Insights from a new cranial reconstruction of the Neandertal newborn from Mezmaiskaya. J Hum Evol *62*, 300-313.

S14. Neubauer, S., Gunz, P., and Hublin, J.J. (2009). The pattern of endocranial ontogenetic shape changes in humans. J Anat *215*, 240-255.

S15. Klingenberg, C.P. (2013). Visualizations in geometric morphometrics: how to read and how to make graphs showing shape changes. Hystrix *24*, 15-24.

S16. Zollikofer, C.P.E., and Ponce de León, M.S. (2004). Kinematics of cranial ontogeny: Heterotopy, heterochrony, and geometric morphometric analysis of growth models. J. exp. Zool. *302B*, 322-340.

S17. Zollikofer, C.P.E., and Ponce de León, M.S. (2013). Pandora's growing box: Inferring the evolution and development of hominin brains from endocasts. Evol Anthropol *22*, 20-33.

S18. Scott, N., Neubauer, S., Hublin, J.-J., and Gunz, P. (2014). A shared pattern of postnatal endocranial development in extant hominoids. Evol Biol *41*, 572-594.